TEST Engineering & Management

July - August 2020
ISSN: 0193-4120 Page No. 5368 - 5377

Automatic Unloading Control of Dump Train Based on Passive RFID Positioning Technology

Zailin Li*
Xinxiang University, Xinxiang, Henan, China, 453003

Article Info
Volume 83
Page Number: 5368 - 5377
Publication Issue:
July - August 2020

Article History
Article Received: *25 April 2020*
Revised: *29 May 2020*
Accepted: *20 June 2020*
Publication: *28 August 2020*

Abstract

The current status and development of dump trains suggest that the unloading system of trains is developing towards automation and intelligence. The positioning system of vehicles has become the key to the unloading system. Passive RFID is characterized by general non-line of sight (NLOS), contactless communication, etc. Passive RFID also has a low cost, excellent reliability, and adaptability to the harsh environment at the unloading site. Hence, the passive RFID system is applicable for the automatic unloading positioning system of hopper dump trains. In this paper, based on the unloading logic requirements of unloading trains, the unloading algorithm in the control system is designed. The composition and basic working mechanism of RFID are analyzed, focusing on the design of the positioning system based on the passive RFID (mainly readers with the RSSI value reading function according to the RSSI acquisition method). The positioning algorithms based on the ranging and non-ranging are analyzed, and the positioning of passive RFID based on RSSI is introduced. For the issue of passive RFID without field strength detection, the field strength detection circuit is designed and analyzed for the tag. Finally, the experimental data are analyzed and simulated, and the factors affecting the accuracy of train positioning are analyzed.

Keywords: *Passive RFID Positioning Technology, Dump Train, Automatic Unloading Control, Measurement;*

1. Introduction

The traditional unloading methods such as back unloading and side unloading have inferior stability, prone to rollover, tires stuck in cargo, and other defects. The hopper unloading train with the bottom opening can solve the defects of the other unloading methods properly. Currently, the automatic unloading train with the bottom opening has become a trend, and the basis of the train unloading control system for train control is the vehicle position. Hence, vehicle positioning has become a crucial issue [1-2]. The radio frequency identification (RFID) features contactless communication, broad identification, intense penetration, and strong anti-interference capacity. In this paper, the unloading system of the hopper unloading train is taken as the background [3-4], and passive RFID is used to perform vehicle identification and positioning. So far, there have been many methods for train positioning, such as magnetic steel, active wheel sensors, infrared sensors, ultrasonic sensors, and GPS positioning [5-6]. However, none of the above methods can be used to identify the vehicle. They also have defects such as the insufficient accuracy of the measurement position, unreliable work, and poor environmental adaptability [7-8].

The application of the RFID technology to the identification and positioning is a new method where communication, identification, and positioning are integrated. It gives the system the advantages of strong anti-interference capacity, simple device, high reliability, and high positioning accuracy [9-10]. RFID can be divided into two categories, active and passive RFID. The practical application system based on active RFID for vehicle positioning is available. However, as active tags require power, the

Published by: The Mattingley Publishing Co., Inc.

July - August 2020
ISSN: 0193-4120 Page No. 5368 - 5377

service life is short, and it is not convenient to apply them to many occasions where power access is inconvenient. The hopper train with the bottom opening adopts a mechanical collision switch door mechanism. The collision mechanism on the ground controls the extension and reset of the collision rod based on the layout of the unloading station. To solve the above control issues, we use many positioning tags in the appropriate parts of the vehicle body. Where active tags are used, it may be difficult to access the power supply or replace the battery. Hence, the passive RFID positioning technology is explored in this paper and applied to the automatic unloading system of the dump train with the bottom opening.

2. Methods

2.1. Operating Principle of the RFID System

RFID technology is a type of radio frequency communication technology. Its contactless and automatic identification and information transmission functions are implemented through the transmission of electromagnetic waves. RFID technology can carry massive information and enable bidirectional data exchange, suitable for identification and information exchange. RFID technology also features non-line-of-sight (NLOS) and contactless communication. The identification and transmission process requires no human intervention. Hence, it has been extensively used with great development potential and application value. The RFID system is generally composed of a reader, electronic tags, an antenna, and a host computer, as shown in Figure 1 below.

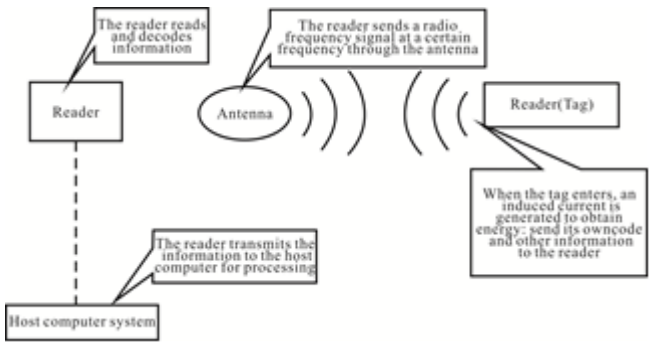

Figure 1. Operating principle of the RFID system

The basic dynamic workflow of a complete RFID system is shown in Figure 2.

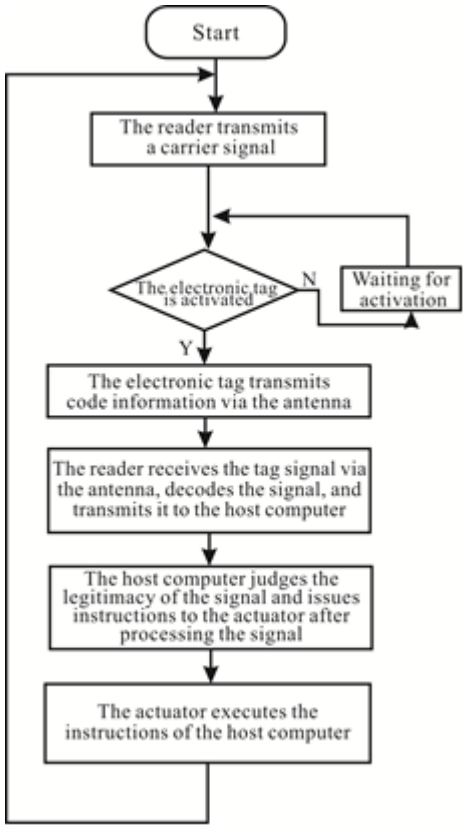

Figure 2. Basic workflow of the RFID system

In the workflow of the whole system, the host computer serves as a data management system that links the entire system and issues the corresponding execution instructions to the actuators based on the needs of different targets to achieve the required control effect.

2.2. Overall Composition and Strategy of the Control System

In the system, the principles of simplicity and reliability are followed, so that the system can meet the requirements of safety, reliability, economic efficiency, and applicability. The whole system is composed of a master control cabinet, AC stabilized voltage supply, DC stabilized voltage supply, a ground collision device drive control box, a collision detector motion detector (reset and setting position detection), a passive RFID travel positioning system, and a remote control communication interface.

Master control cabinet: The master controller adopts a highly reliable PLC to collect the

Published by: The Mattingley Publishing Co., Inc.

July - August 2020
ISSN: 0193-4120 Page No. 5368 - 5377

positioning, vehicle, and other related signals to complete the entire control logic. Its work can be divided into two parts, the automatic and manual parts, which are set through the switch. The on-site working status (collider reset/set status, alarm, and so on) can be displayed on the master control panel. The master control cabinet is equipped with manual control buttons.

AC stabilized voltage supply: As the AC power supply on-site is not stable, AC stabilized voltage supply shall be added.

DC stabilized voltage supply: Readers and station controllers are provided on-site, which require DC power and are installed inside the master control cabinet.

Collider drive box: It adopts the hydraulic drive control and is installed in a proper position near the collision device, convenient for resetting/setting the collision device.

Collider motion detection: It is completed through a proximity switch. The system can detect whether the collider is operating based on the instructed actions. The setting is required at this position; otherwise, the goods will not be unloaded. In addition, the reset should be performed as required; otherwise, an accidental collision may occur and lead to an accident.

Positioning system: The positioning system is the key system. The passive RFID system is used to locate the vehicle travel. The passive RFID reader can detect echo RSSI.

The overall frame architecture of the system is shown in Figure 3.

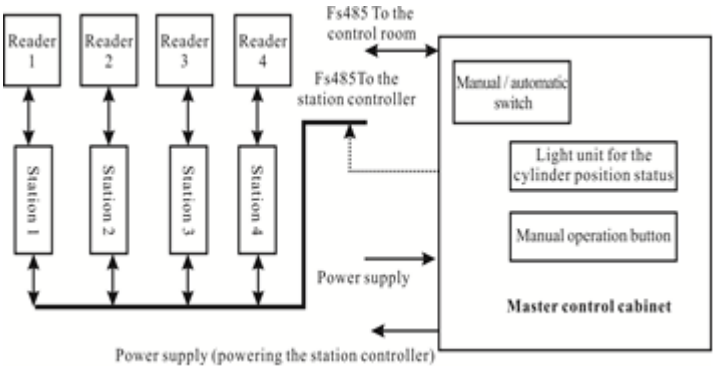

Figure 3. Block diagram of the system hardware architecture

The key to the success of the system is the control strategy, i.e., the vehicle positioning is implemented through the passive RFID system, where the vehicle is counted, and the PLC master controller is provided with a reliable vehicle position and vehicle identification signal. The PLC is used to complete the control algorithm, thereby implementing the unloading function as required. The operating principle of the passive RFID system is that when the wheel of the vehicle passes the reader, the reader emits an electromagnetic field signal to the passive tag, and reads the ID information of the tag on the vehicle. The ID can be used to identify the locomotive/non-locomotive. The locomotive tag count can be used to identify the number of cars. The flow chart for the control strategy algorithm of this system is shown in Figure 4.

Published by: The Mattingley Publishing Co., Inc.

July - August 2020
ISSN: 0193-4120 Page No. 5368 - 5377

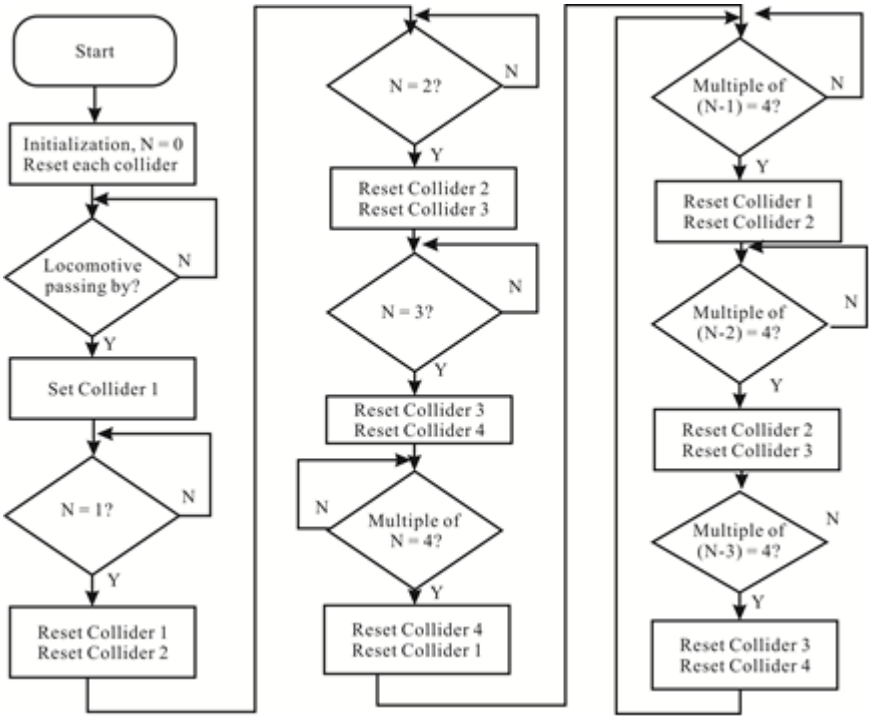

Figure 4. Unloading process based on the passive RFID system

The algorithm shown in Figure 4 is a control strategy composed of a PLC controller and four stations. PLC should communicate with four readers at the same time. The counting is required, and then the algorithm is performed to complete the control of the four stations. To increase the reliability of the system and the simplicity and generality of the algorithm, we design the corresponding control algorithm based on the station. As the station is fixed, each station works independently, and each station is numbered (N = 1,2,3,4). The switch control time of the corresponding collision is different.

2.3. Design and Selection of Hydraulic Components

The traditional dump train is generally designed with a lifting angle of 45°. The tipping chassis is used to transport bulk goods and can load multiple types of materials. Some loose materials, such as sand, gravel, and grain, have excellent fluidity. The angle of repose is generally around 38°, where the angle of repose is usually around 38°. In general, the angle of repose at about 45° in the tipping chassis is selected. However, some materials, such as clay and wet ore powder, have a larger angle of repose. Hence, it is required that the dumping lift angle of the cargo compartment in the dump truck should be 50° ± 5° for material dumping. Therefore, the angle of repose for the dump trailer should be greater than 50°. In this design, 55° is selected, i.e., the tilt angle is 55°.

Given that the static friction torque of each hinge point at the initial stage of lifting is large, to ensure the smooth working of the hydraulic system and avoid excessive shocks, the torque ratio coefficient η (η represents the ratio of the lifting torque provided by the lifting mechanism to the resistance) is introduced, and η = 2.

Based on the type of the host, the working pressure of the actuator is selected. As required by the specifications, the conditions of the hydraulic components, and the use of the vehicle, the working pressure *p* of the hydraulic system is 16 MPa.

1) Calculate the lift force F of the cylinder at the first stage

Through the analysis of the stress on the cargo compartment, the maximum lifting force of the lifting cylinder indicates that when the compartment is just lifted, as the lifting of the compartment continues, the lifting force becomes increasingly small.

$$F_{\max} \times \cos\varphi \times L = \eta \times G \times L_1 \quad (1)$$

Published by: The Mattingley Publishing Co., Inc.

July - August 2020
ISSN: 0193-4120 Page No. 5368 - 5377

Where F_{max} represents the maximum lifting force of the lifting cylinder; φ represents the installation angle of the cylinder (°); the installation angle of the vehicle is 15°; L represents the horizontal distance from the rear support point of the compartment to the lower hinge point of the lifting cylinder; L_1 represents the horizontal distance from the center of gravity to the support point behind the compartment; η represents the torque ratio coefficient; G represents the sum of the load mass and the compartment mass (kg).

Thus, the maximum thrust of the cylinder can be obtained as follows:

$$F_{max} = \frac{\eta \times G}{2 \times \cos\varphi} = \frac{2 \times (30000 + 8000)}{2 \times \cos 15°} = 36705kg \quad (2)$$

Based on the available cylinder parameters, $F_{max} = 44$ t is obtained.

2) Calculate the diameter of the cylinder

The working diameter D_1 of the first telescopic cylinder is obtained from the thrust $F = \frac{\pi D^2}{4} \times p$ of the cylinder as follows:

$$D_1 = \sqrt{\frac{4F_{max}}{\pi \times p}} = \sqrt{\frac{4 \times 44 \times 103 \times 9.8}{\pi \times 16 \times 106}} = 185.28 \text{ mm} \quad (3)$$

3) Calculate the total stroke S of the cylinder

$$S_{max} = \sqrt{OA^2 + OB^2 - 2 \times OA \times OB \times \cos\theta_{max}} = 7089 \text{ mm} \quad (4)$$

Based on the overall installation pattern, the installation center distance of the lifting cylinder is as follows: S_0 = AB = 350 mm. The total stroke S of the lifting cylinder can be obtained:

$$S = S_{max} - S_0 = 7089 - 350 = 6739 \text{ mm}$$

Based on the above parameters, the lifting cylinder selection model is FC-190-5-07130-000A-K0343, and its overall parameter requirements are as follows: The total capacity of the oil cylinder is 140 L, the effective diameter of the first section of the cylinder is 190 mm, the total stroke is 7130 mm, and the number of levels is 5, which can meet the requirements. The hydraulic cylinder has a built-in limit valve, which can control the maximum stroke of hydraulic lifting. Meanwhile, it has a ramp down function that allows the compartment to land slowly when it declines and gets close to the frame, thereby reducing the impact and achieving a high cycle speed, excellent resistance to high pressure, and a long service life.

Given that a hydraulic pump will lead to a relatively large area of the oil return and pipeline, the economic benefit is not ideal. Besides, the waste of materials is relatively severe. Hence, a double gear pump is used in the proposed, which can save materials and reduce the costs effectively.

The flow of oil through the lift cylinder is significantly higher than that through the motor. In addition, the lifting cylinder and the motor rotate at different times. Thus, the flow rate of the pump depends on the flow rate of the lifting cylinder.

The time for lifting the compartment to 55° is t ≤ 40s, and 1.1 is taken for the leakage coefficient K of the system.

As required by the mission statement, the lifting and lowering time should be t ≤ 40s, and the multi-stage telescopic oil cylinder of a company is adopted. Its working volume is V = 140 L, and the flow rate Q of the oil pump is as follows:

$$Q = \frac{K \times V}{t} = \frac{1.1 \times 140}{40} = 3.85(L/s) \quad (5)$$

As the power of the pump comes from the gearbox of the tractor, the rated speed n of the pump is 2000 r/min.

The displacement of the pump is as follows

$$q_p \geq K \times \sum Q_{max} = \frac{Q}{n} = \frac{3850}{2000} \times 60 = 115.5(\text{mL/r}) \quad (6)$$

At this point, the CB-G3125 double pump is selected.

The working pressure of the primary hydraulic motor is 4 MPa; the load is 1000 N; the diameter of the reel is 100 mm; the load torque T of the motor is 50 N.m.

According to the following equation

Published by: The Mattingley Publishing Co., Inc.

July - August 2020
ISSN: 0193-4120 Page No. 5368 - 5377

$$V_m = \frac{2\pi T}{\Delta p \eta_m}$$

the displacement of motor can be obtained as follows:

$$V_m = \frac{2\pi T}{\Delta p \eta_m} = \frac{2 \times 3.14 \times 50}{4 \times 10^6 \times 0.9} = 87.2(\mathrm{mL/r}) \quad (7)$$

Where Δp represents the difference in the working pressure between the two chambers of the motor; η_m represents the mechanical efficiency of the motor.

3. Results

The experiment of this system is completed on a single-channel passive RFID system, where the UHF read-write module by Shenzhen Jiurui Technology Co., Ltd. is used, as shown in Figure 5. The 6c standard passive tags are used (the 12dB UHF directional antenna is shown in Figure 6). The experimental setup is shown in Figure 7, where the directional antenna is fixed. The passive tag is installed on a movable object so that the tag reading and writing operations of the reader can be performed within its reading range.

Figure 5. UHF RFID reader

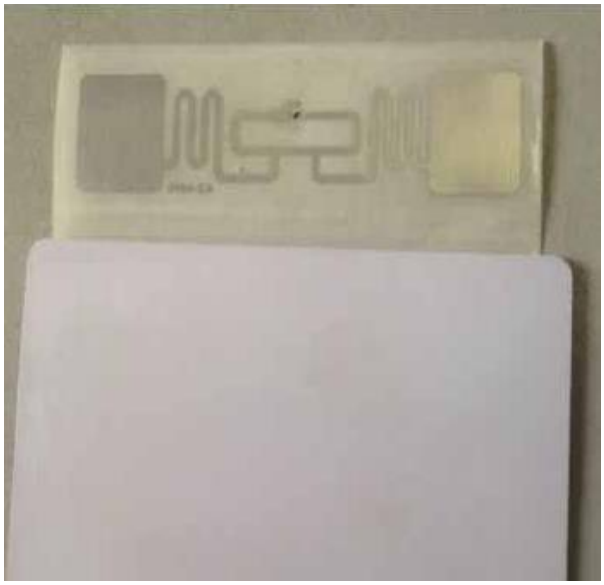

Figure 6. RIFD 6C passive tag

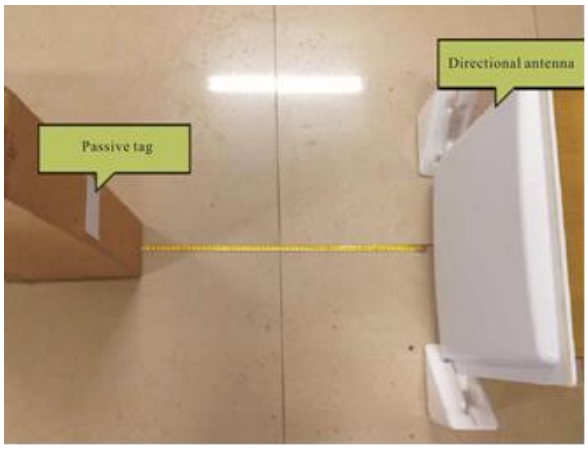

Figure. 7 Experimental setup

The passive tag is installed at the same height as the geometric center of the antenna, and the tag movement direction is perpendicular to the directional antenna. The RSSI value is currently recorded at an interval of every other 0.l m. As the reader reads the RSSI of the tag, the RSSI value displayed at a fixed point is not fixed but fluctuates within a small range. Hence, the mean value of multiple records is taken as the field strength value at that point. The data are shown in Table 1 as follows.

Table 1. RSSI value record table

Position (m)	0.4	0.5	0.6	0.7	0.8	0.9	1.0	1.1	1.2	1.3
RSSI	-46.75	-46.0	-47.0	-48.33	-49.0	-49.67	-50.33	-50.67	-51.33	-52.0

Published by: The Mattingley Publishing Co., Inc.

July - August 2020
ISSN: 0193-4120 Page No. 5368 - 5377

(dBm)										
Position (m)	1.4	1.5	1.6	1.7	1.8	1.9	2.0	2.1	2.2	2.3
RSSI (dBm)	-52.0	-53.0	-53.0	-53.67	-54.0	-64.67	-56.0	-56.67	-57.67	-58.0
Position (m)	2.4	2.5	2.6	2.7	2.8	2.9	3.0	3.1	3.2	3.3
RSSI (dBm)	-58.67	-60.0	-58.67	-61.67	-60.33	-63.67	-61.0	-64.25	-63.67	-64.0
Position (m)	3.4	3.5	3.6	3.7	3.8	3.9	4.0	4.1	4.2	4.3
RSSI (dBm)	-68.0	-63.33	-65.0	-66.33	-66.0	-66.0	-67.33	-68.33	-70.0	-70.5
Position (m)	4.4	4.5	4.6	4.7	4.8	4.9	5.0			
RSSI (dBm)	-72.5	-67.0	-72.0	-73.67	-70.67	-72.67	-68.33			

After the curve fitting is performed on the obtained RSSI value in the MATLAB, as shown in Figure 8, it can be seen from the figure that the RSSI value received by the reader as a whole is in a decaying trend within the range of 0.4 m to S m from the vertical distance of the reader within 0.4 m ~ 2.5 m, where the RSSI value decreases one by one. However, after 2.5 m, some RSSI values present non-decaying bounce, which is an unreasonable RSSI value due to the uneven distribution of field strength caused by the measurement environment. Hence, the variation pattern of RSSI values is entirely consistent with the theory.

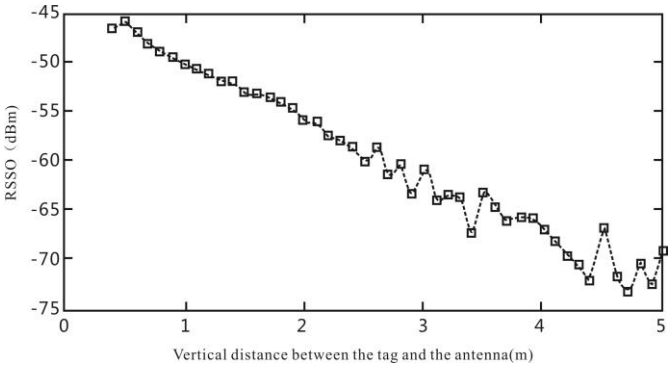

Figure 8. Change curve of RSSI with the distance

Figure 8 shows that the change of RSSI is relatively regular within 0 – 2 m. At a farther measurement distance, the actual measurement will present the jump of RSSI value. Hence, it is important to select the appropriate range. In the subsequent experiments, the vertical distance of 1.6 m is selected as a benchmark for the measurement.

The appropriate vertical distance L between the tag and the antenna is selected. The intersection point with the trajectory of the tag at the distance L is taken as the origin and coordinates (0,0). The current RSSI value (or the distance measured by the algorithm) is recorded every other 5 cm, and the ranging algorithm is used to implement the positioning.

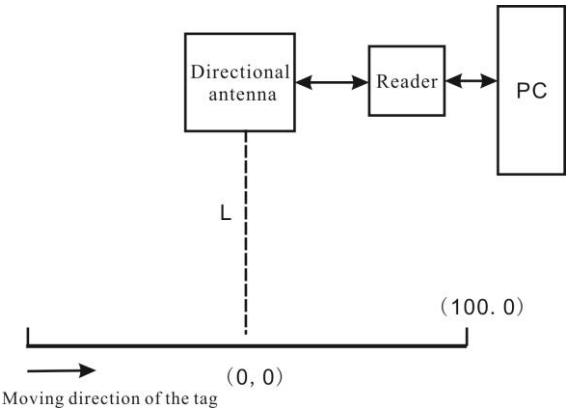

Figure 9. Simulated train travel positioning

Based on the method shown in Figure 9, a coordinate origin is established at a distance of 160 cm from the directional antenna. The tag transport

Published by: The Mattingley Publishing Co., Inc.

July - August 2020
ISSN: 0193-4120 Page No. 5368 - 5377

direction is along the X-axis, and the perpendicular line between the antenna and the movement direction is along the Y-axis. The tag is moved from the X-axis (from -100,0 to (100,0) at an interval of 5 cm each time to simulate the stroke movement of the unloading train, and the RSSI value returned by the current tag from the reader is recorded (the mean value of multiple measurements is taken), as shown in Table 2.

Table 2. Experimental data of the positioning

Coordinate	(-100,0)	(-95,0)	(-90,0)	(-85,0)	(-80,0)	(-75,0)
RSSI	-62.33	-60.33	-59.33	-58.33	-58	-57.67
Coordinate	(-70,0)	(-65,0)	(-60,0)	(-55,0)	(-50,0)	(-45,0)
RSSI	-57	-66.67	-56	-55.33	-54.67	-54.33
Coordinate	(-40,0)	(-35,0)	(-30,0)	(-25,0)	(-20,0)	(-15,0)
RSSI	-53.33	-53	-53	-52.67	-52.67	-52.33
Coordinate	(-10,0)	(-0,0)	(0,5)	(0,10)	(0,15)	(0,20)
RSSI	-52	-52	-52	-52	-52.67	-53
Coordinate	(0,25)	(0,30)	(0,35)	(0,40)	(0,45)	(0,50)
RSSI	-53.33	-54	-54.33	-54.67	-55.33	-55.67
Coordinate	(0,55)	(0,60)	(0,65)	(0,70)	(0,75)	(0,80)
RSSI	-56.67	-58	-59	-61	-62.33	-63.37
Coordinate	(0,85)	(0,90)	(0,95)	(0,100)		
RSSI	-65.33	-67.33	-66	-66.73		

The corresponding coordinate point is selected from Table 2. The change in the linear distance of the corresponding coordinate point and the geometric center of the antenna from the tag displacement is obtained according to the distance calculation formula (where the appropriate propagation factor and random component are selected), as shown in Figure 10.

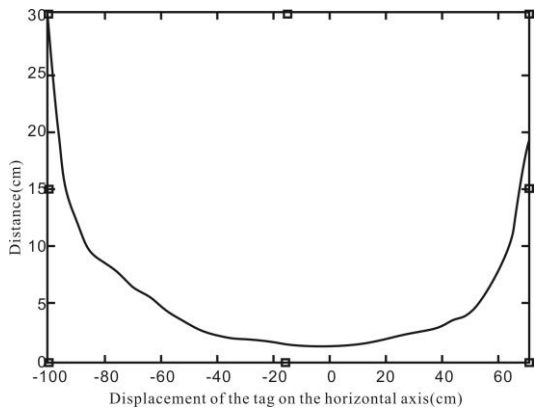

Figure 10. Simulated driving distance measurement value

The figure shows that the change law for the measured distance conforms to the changing relationship between the tag motion law and the distance. To complete the positioning, we need to select an appropriate reference distance. The experiment shows that within the range of (-10,0)-(10,0), the measurement distance is constant, and its value is 1.5983 m, which is the shortest. If the coordinate origin is selected as the reference location point, it can be known from the ranging positioning algorithm that where the distance difference is C = O, the point where the measured distance is less than or equal to the measured distance between the reference point and the tag for the first time should be the point, and the error is 0. The appropriate reference position point is selected (i.e., a suitable antenna installation position is selected), where the positioning accuracy will also be changed accordingly. A different reference position point is selected, and the change in the RSSI is observed when the tag is moved gradually at this point. The ranging formula is used to calculate the relative distance between the changing point and the reader. Subsequently, the point where the measured distance is greater than or equal to the reference point (c = 0)

Published by: The Mattingley Publishing Co., Inc.

July - August 2020
ISSN: 0193-4120 Page No. 5368 - 5377

for the first time is obtained based on the positioning algorithm, i.e., the positioning point. In this system, the train movement rate is 33 cm/s only, when the reader can read the tag up to 60 times in the is. In addition, the mean value of four reads is taken by the controller in this system, and 15 values can be obtained. Hence, the error correction value of 2.2 cm should be added. The relative error between the reference point and the positioning point is calculated, as shown in Table 3.

Table 3. Ranging positioning error

Reference positioning coordinate	(-50,0)	(-45,0)	(-40,0)	(-35,0)	(-30,0)	(-25,0)
Positioning point	(-46,0)	(-46,0)	(-34,0)	(-34,0)	(-25,0)	(-21,0)
Relative error (cm)	6.2	3.2	8.2	3.2	7.2	6.2

From Table 3, it can be seen that the ranging positioning can be used to control the relative error within 8.2cm for the one-dimensional travel moving target. The key to the error control is to install the antenna and the tag to ensure the proper position between them and apply a reasonable algorithm.

4. Conclusions

With the continuous rise and development of RFID technology, its application fields have become increasingly extensive. The RFID technology features non-line-of-sight (NLOS), contactless, identifiable, massive data storage, and bidirectional data exchange. In terms of positioning, it has great advantages in the economy, positioning accuracy, and other performances compared with GPS positioning technology, ultrasonic positioning technology, Bluetooth technology, UWB technology, etc. In this paper, the positioning system of the hopper dump train is designed, and the traditional wheel sensor is used as the system positioning algorithm. The defects of this method are pointed out. It is proposed that the passive RFID should be used for the positioning system of the dump train, and the corresponding algorithm is designed. In general, the algorithms can be divided into the ranging and non-ranging positioning algorithms. The relevant ranging methods are analyzed. Finally, two methods based on RSSI ranging and non-ranging are used for system positioning. The important part at the front end of the passive RFID reader is designed and analyzed accordingly.

References

[1] Enrique Valero, Antonio Adan, & Carlos Cerrada. (2012). Automatic construction of 3d basic-semantic models of inhabited interiors using laser scanners and rfid sensors. Sensors, 12 (5), 5705-5724.

[2] S.-W. Huang, M.-T. Lee, & D.-C. Gong. (2011). Implementing a passive rfid e-seal system for transit container security: a case study of kaohsiung port. Advances in Transportation Studies, 26 (26), 69-88.

[3] Wang, J., & Katabi, D. (2013). Dude, where's my card?: rfid positioning that works with multipath and non-line of sight. Computer Communication Review, 43 (4), 51-62.

[4] Fu Xiao, Zhongqin Wang, Ning Ye, Ruchuan Wang, & Xiang-Yang Li. (2017). One more tag enables fine-grained rfid localization and tracking. IEEE/ACM Transactions on Networking, PP (99), 1-14.

[5] Sen Zheng, Kai Cheng, Jixin Wang, Qingde Liao, & Weiwei Liu. (2015). Failure analysis of frame crack on a wide-body mining dump train. Engineering Failure Analysis, 48, 153-165.

[6] Dong Cui, & Qiang Zhang. (2017). The rfid data clustering algorithm for improving indoor network positioning based on landmarc technology. Cluster Computing (5), 1-8.

[7] John Edwards. (2017). New directions in

Published by: The Mattingley Publishing Co., Inc.

July - August 2020
ISSN: 0193-4120 Page No. 5368 - 5377

navigation and positioning: signal processing-enabled technologies pinpoint people, places, and things [special reports]. IEEE Signal Processing Magazine, 34 (3), 10-13.

[8] Razia Haider, Federica Mandreoli, & Riccardo Martoglia. (2014). Rpdm: a system for rfid probabilistic data management. Journal of Ambient Intelligence and Smart Environments, 6 (6), 707-722.

[9] Andreas Stelzer. (2010). Ieee international microwave workshop series on wireless sensing, local positioning, and rfid [around the globe]. IEEE Microwave Magazine, 11 (1), 105-106.

[10] X. Zhao, J. Yang, W. Zhang, & J. Zeng. (2015). Sliding mode control algorithm for path tracking of articulated dump train. Nongye Gongcheng Xuebao/transactions of the Chinese Society of Agricultural Engineering, 31 (10), 198-203.

Published by: The Mattingley Publishing Co., Inc.